

Final Report

DROP TUBE TECHNICAL TASKS

(NASA-CR-178741) DROP TUBE TECHNICAL TASKS  
Final Report (Alabama Univ., Huntsville.)  
44 p HC A03/MF A01 CSCL 14B

N86-21564

Unclas  
G3/12 16596

---

# Kenneth E. Johnson Environmental and Energy Center

---



The University  
Of Alabama  
In Huntsville

---



January 1986

UAH Research Report No. 475

Final Report

DROP TUBE TECHNICAL TASKS

Submitted to

NATIONAL AERONAUTICS AND SPACE ADMINISTRATION  
George C. Marshall Space Flight Center  
Marshall Space Flight Center, Alabama

Contract No. NAS8-35665

Submitted by

A handwritten signature in cursive script, reading "Gary L. Workman", is written over a horizontal line.

Gary L. Workman, PhD  
Principal Investigator  
Johnson Environmental and Energy Center  
The University of Alabama in Huntsville  
Huntsville, AL 35899

January 1986

## Acknowledgements

I appreciate the efforts of many persons in the performance of this work. In particular, Dr. William F. Kaukler, who was extremely helpful in performing the metallurgical aspects of this project and for his leadership in performing the drops. Steve Straits and his colleagues at the Drop Tube did an exceptional job of getting drops whenever possible. Also to Dr. Ed Etheridge for his efforts as technical contract monitor.

## I. Introduction

The Drop Tube Facility at Marshall Space Flight Center is a national asset used for studying a variety of solidification phenomena in a low gravity environment or as a containerless processing system. By virtue of the relatively short turn around times required to assess experimental parameters, it is possible to learn much about a particular experiment and possibly its behavior as an experiment aboard the space shuttle or space station, without leaving the ground. A unique facility of this type requires a large amount of resources available to perform the experiments, maintain the equipment and to provide useful information in order to design a good experiment.

The objective of this study was to develop criteria, using fundamental thermochemical dynamics, to assist a scientist using the Drop Tube Facility in designing a good experiment. The types of parameters involved in designing the experiments include the type of furnace, the type of atmosphere, and in general which materials are better behaved than others as determined by past experience in the facility. One of the major advantages of the facility lies in its ability to provide large undercoolings in the cooling curve during the drops. The ability to predict such undercoolings has not progressed due to the lack of information with most systems and lack of a suitable theory to predict such behavior. Consequently, we felt that a good beginning was to consider the effect of oxygen and other gases upon the amount of undercooling observed. The starting point of the thermochemistry was given by Ellingham<sup>1</sup> and later transformed into what is known as the Richardson Chart (Figure 1).<sup>2,5</sup> Having the local capability to calculate such quantities presented an early

objective. In addition data was to be obtained from experimental drops of elemental species, in order to observe the effect of surface oxidations upon the nucleation phenomena observed in each specimen.

## II. Results

The thermochemical calculations for the free energies of formation have been programmed on two different computers available to drop tube personnel. The first version was programmed using the IBM personal computer and a later version was programmed on the Hewlett-Packard 9836 in the Drop Tube Facility on the 15th floor. This report contains the IBM version of the program, as well as several of the outputs, as Figure 3-6 and Appendix A. The thermodynamics used for the calculation is given in Figure 2. Data is taken from References 3 and 4. A major advantage of using local calculation capability over just extrapolating from Figure 1, is that as newer data becomes available in terms of materials and phase transitions, the drop tube user will be able to determine the thermochemistry more appropriately for his circumstance. Also it is envisioned that the gas effects will be extended to handle many more species in the future. Figures 3-6 show program flow, data presentation screens for NiO and NiO plot from IBM-PC.

The drops performed for this study are included in Tables I-III. In addition, information is given in terms of the mass, the observations performed and the resulting grain or dendrite measurements. As indicated later, we were not able to correlate the surface oxide formation with amount of undercooling, but we did establish that a new parameter needed to be considered for a better understanding of the resulting microstructures.

Gas solubility, not considered previously as important as oxide formation does show in our microstructure analysis that the morphology was affected more by varying ambient atmosphere than by surface oxidation effects. We still have not finished analyzing the specimens obtained during these drops, but Tables I-III summarize the data obtained thus far fairly completely.

A major undertaking of this effort has been the microstructural analysis performed by Dr. William Kaukler who has been extremely active in similar work with low gravity experimentation from drop tower and KC-135 studies. Dr. Kaukler has been assisted by Ms. Donna Warden, an undergraduate student at UAH in performing most of the grinding, polishing and photomicroscopy for the same studies. As seen in Table I, we have used specimens of copper, rhodium, platinum, and nickel. The only reason for using these elements were due to their availability and as far as we knew at the beginning of this work, they were not being worked by other research groups in cooperation with NASA.

### III. Discussion of the Results

This discussion is presented to provide information about the type of information obtained from these sets of experiments. The breakdown can be classified according to the following areas:

- Specimen Preparation for Metallography

- Photomicrography of Specimens

- Residual Gas Analysis

- Analysis of Dissolved Gases

- Summary of Etching Procedures

The complete interpretation and analysis will take some time to finalize. We hope that this preliminary information will be of use to other scientists who are interested in using the Drop Tube in studies of solidification phenomena.

#### IV. Drop Tube Specimen Preparation for Metallography

Over 60 drop tube specimens were mounted, sectioned by grinding, polished and analyzed metallographically. Tables 1-3 list the drop specimen parameters. Some specimens revealed microstructural details on their exterior surfaces. These specimens were examined by scanning electron and optical metallography prior to mounting and sectioning. Practically all the experimental results are derived from these metallographic studies. Microstructural correlations to the drop conditions are the prime observations. Photomicrograph of several interesting specimens are given in Figures 8-10.

Specimens were as small as 20 milligrams in weight for the electron beam experiments and 200-400 milligrams for the electromagnetic levitation experiments. Such small samples represented considerable difficulty in handling and in the proper performance of metallographic sectioning. All specimens were near perfect spheres and the considerable surface curvature made microscopic examination of exterior features nearly impossible. Surface features were of considerable interest to this study because normal shrinkage of the melt upon crystallization can reveal dendritic morphology, which may yield details of its thermal history. No correlation would or could be made between the site of apparent nucleation on sectioning and the surface morphology. Dendrite arm spacing, if found on the surface could be compared to the spacing, if seen, in the interior region of the specimen.

Most of the time consumed for this study was spent on the systematic development of the various metallographic techniques required to produce acceptable micrographs of the diverse specimen types. Many of the specimens were soft metals which were further softened by their high purity. Soft specimens scratch very easily, are deformed, are susceptible to surface deformation during mechanical polishing, provide little resistance to machining, retain grinding and polishing abrasives by embedding into the surface and cause other minor problems during metallographic analysis. In order to minimize these difficulties, the specimens were individually mounted and had embedded with them in the mount, a ring of glass around the specimen. This ring stabilizes the orientation of the specimen, greatly improves the characteristics of the polished specimen, and permits a less skilled metallographer to achieve superior results.

Each different metal that was studied required its own procedure for preparation. Mounting, grinding, and in general most polishing tasks were done the same way, but skill was required in order to develop and repeat the proper application of these steps. A variety of specimen etching techniques had to be attempted despite the ready availability of previously tested formulas and methods collected in reference texts. The specimens selected for this study were prepared from the most pure elements available. This leads to the most complicated feature of the metallographic studies. When a metal is very pure, morphological features formed during crystallization will not leave clear traces of their passing; whereas common alloys always leave a clear trace of their passing. These features can become undetectable to any method. Nearly always does grain recrystallization occur unimpeded by the pinning effects on grain boun-

daries of solute atoms. Prior structure usually could not be revealed, although dendrite arm spacing measurements on occasion could be made. The heat of recalescence and the slow cooling rates after crystallization together with the high purity enhance the rate of grain growth. At the very least, grain structures could be revealed by some etching techniques. Again the high purity and nobility of some of the elements studied required concentrated effort to find acceptable etchants. If chemical etchants were not successful, some success was obtained with electrolytic etching methods. A facility for electro-etching of metal specimens was established as a result of this requirement (See Figure 11). The high nobility of some of the metals required aggressive techniques for etching. Therefore, the only microstructures revealed were the grain boundaries. Summarized in this report are also the best etchants and additional cautions for such elements studied.

All the specimens had to be mounted in plastic "cold mount" prior to grinding. The best material was found to be a product from SPI, a polymethyl methacrylic material. Specimen mounts were standard metallurgical types, approximately 30 mm. in diameter.

Grinding was performed wet with tap water as the lubricant. Wet/dry grinding papers with corundum grit were used with the standard sequence of 120, 180, 230, 420, and 600 grit for all specimens.

Mechanical polishing was performed at first with alumina polishing suspensions in water having particle sizes of 5, 1, 0.3 micrometers. Coarse and then fine polishing was always performed with billiard cloth for the fine polish and "Super Finale" cloth for coarse. For the latter half

of the study, a more expensive and troublesome diamond polish was performed. Surface finish was superior and polishes were done more quickly, but scratches were always found and highly revealed by the etching process. Both coarse and fine diamond polishing was performed with 1 and 0.25 micrometer diamond particles used in a suspension of diamond polishing oil. The best cloth was found to be "Rayvel" from Beuhler for both grit sizes.

Copper was prepared by the first mechanical polishing followed by a chemical polish prior to the chemical etch. The chemical polish removed the scratches of the mechanical polish and produced a superior surface. The formula is included together with the etchants.

#### V. Photomicrography of Specimens

Metallographic examination of the drop tube specimens combined exterior observation by optical and electron microscopy with micrography of the polished and etched sections. The features which were examined for included dendrite size and spacing, surface oxidation, grain size, porosity, and sites of nucleation if found. The dimensions of these features are such that only low magnifications are required. Given the dimensional range, more stereological measurements per micrograph can be made for the lower magnifications, thus providing improved statistics.

A Zeiss Ultraphot Research Microscope and Unitron U-11 Metallograph were used for optical metallography. A Jeol UM-3 Scanning Electron Microscope was also used for surface examination. Nearly all the metallography centered around the micrography of polished and etched sections of the drop tube specimens. When photographs were taken with the Zeiss microscope, either Polaroid type 58 film (color) or type 57 film

(black and white) was used, and with the Unitron, Polaroid type 108 or 107 film was used. Kohler, bright field illumination was used in most cases. Occasionally, when polished but unetched specimens were studied, Nomarski interference contrast illumination was used to reveal the subtle variations in surface texture. Surface examination and optical photomicrography were done using dark field illumination on the Zeiss microscope. This type of lighting enhances the contrast for the very rough structures, sometimes seen due to solidification shrinkage in interdendritic cavities.

All the special lighting techniques are available on the Zeiss microscope. Three objective lenses yield three different magnifications; 40X, 65X, and 260X. Only Kohler illumination was available with the Unitron U-11 and all micrographs were taken with the 10X objective, resulting in a 136.5X magnification in the photomicrograph.

Except when Nomarski illumination was used (which creates a pseudo-color image), the specimens showed no color. As a result black and white micrographs were taken of these specimens. The exception is the copper specimens which, when etched, revealed various shades of orange and brown. Some color micrographs were taken of these.

## VI. Residual Gas Analysis

Knowledge of the quality of the atmosphere in the drop tube environment is critical for studies of this nature. The partial pressures of the significant gaseous species; oxygen, hydrogen, water, carbon monoxide, helium and carbon dioxide collectively can control the chemical potential for reaction at the elevated temperatures used with these types of materials. Either oxidation or reduction of the metal could be per-

formed during its fall through the ambient atmosphere within the tube by suitable gas selection. Even a high vacuum (less than  $10^{-6}$  atmospheres) can contain enough oxygen or water vapor to cause some reactive metals to oxidize significantly. Quantification of the amount of these gases can most easily be performed with a residual gas analyzer or mass spectrometer. In our study, a UTI 100C quadrupole was borrowed from another group and used in the earlier phases of the study, but it was an older system and had many problems in providing data when required. Consequently the Drop Tube Facility purchased a Dycor Electronics M/100M series quadrupole mass spectrometer for dedicated use at the facility. This unit was installed at the top of the tube, in the belljar region above the isolation valve. This unit has a mass range of 1 to 100 amu and utilizes an electron multiplier, thus allowing us to make sensitive partial pressure measures of gases and vapors. Other features of this particular model includes programmed computer control, large CRT display, and printer output of display information. Various display formats are available, including analog, bar representation, tabular, etc.; enabling the data to be displayed a number of different ways.

## VII. Performing Residual Gas Analysis on the Drop Tube

The Dycor quadrupole mass spectrometer has been installed into the belljar region using a scheme which allows the bell jar region to be monitored at both low and high pressure regimes. Two different valves for controlling the sampling parameters of the tube are used in this scheme. A variable leak valve, which allows sampling at very high pressures, is available for pressures above  $10^{-4}$  atmospheres and for pressures below that value a manually operated gate valve is available. Using these two valves

the quadrupole is capable of operating over a very large dynamic range. Under the conditions of our measurements, we used the same turbomolecular pump that pumps on the belljar region to pump out the quadrupole region. A major disadvantage of this approach is that the maximum sensitivity of the instrument is not achieved because the sensing environment is not at a lower pressure than the environment being sensed. We have since then installed a Cryogenic pumping system in order to attain pressure values for the quadrupole region to be much less than for the belljar region. In particular it is important to clean up the water vapor if we are to measure it correctly.

For our measurements, we used a value of 125 for the setting on the variable leak valve and systematically stayed with that leak rate. No actual measurement of the leak rate was made since we did not have the cryogenic pump installed and such a measurement would have been difficult. Working with ratios of known gaseous components is sufficient in most cases. In operation, the use of the variable leak valve allowed a controlled leak from the belljar region into the quadrupole region to occur. The continuous stream of gas passed through the ionizer region of the mass spectrometer chamber being pumped upon by the turbomolecular pump. In this way we were able to obtain scans of the belljar atmosphere under prescribed conditions. An example of such a scan is given in Figure 11. A noticeable feature of the scans obtained with this system is that the peak heights are influenced by two parameters not built into the software controlling the display information. One parameter is the efficiency of ionization (and associated cracking pattern) and the other is mass discrimination effects of both the variable leak valve and the mass spectrometer

itself. This type of variable leak valve uses the volume between two cylindrical surfaces to determine the leak rate and provides a difference in leak rate by varying the overlap region of the two cylinders.

Unfortunately this technique does give some mass discrimination and small molecules such as helium and hydrogen do leak at a proportionately higher rate than larger molecules. This can be calibrated and to some extent compensated for, as can other types of mass discrimination once their causes are identified.

#### VIII. Dissolved Gases

As indicated earlier the major objective of this project was to determine the effect surface oxides would have upon heterogeneous nucleation in undercooled pure metal droplets. This study has indicated that the proper approach is to also account for the effect of gas solubilities, in addition to the chemical reactivity of the various gases present in the atmosphere of the drop tube. Redox reactions and the oxides that result are not the only gas related effects upon the microstructure. Free energies of formation of these oxides and their sensitivity to temperature and pressure were discussed earlier in this report. During the examination of the specimen sections fine dispersions of porosity were found within many of the specimens. The morphology of these pores indicate that they formed as a result of the nucleation of dissolved gas throughout the melt upon cooling. Many specimens show the formation of these pores occurred in the liquid that was last to solidify in the interdendritic regions. The porosity often outlined the interdendritic regions and thus verifies that they resulted from the segregation or partitioning effect of the advancing solidification front.

The cleanliness of these pores prevents a direct assessment of the gas species which caused their formation, hence we felt that a survey of the data for gas solubility was the next best approach order to select the best candidate. One must also recognize that the formation of oxide does not indicate lack of solubility of the oxygen in the melt since solubility measurements do not always preclude a reactive mechanism at work. For porosity to form most readily the solubility fo the gas in the solid should be significantly lower than in the melt. In addition, adequate partial pressure of the gas would be required to cause the solution of the gas. In the experiments presented here, the small droplet sizes with their high surface to volume ratios and the high temperatures within the furnace region would ensure rapid solution.

Three elemental gases can be considered that could cause the porosity observed. They are hydrogen, oxygen and nitrogen. Both oxygen and hydrogen also may go into solution from dissociated water vapor that is always in the drop tube atmosphere. The noble gases helium and argon do not dissolve in any metal to a measurable degree. Sievert's Law applies with hydrogen at least

$$S_a = k\sqrt{P_a} ;$$

solubility being proportional to the partial pressure of the gas.

A summary of data discussed in reference gives us the following information.

Nitrogen is insoluble in the following metals up to 1400 C. for the following three metals:

Copper  
Nickel  
Palladium.

Hydrogen is soluble in the following metals:

- Copper - .03 atomic percent at melting point for liquid  
.009 atomic percent at melting point for solid
- Nickel - 0.1 atomic percent at 1453 C solid  
0.2 atomic percent at 1453 C liquid
- Platinum - low solubility  
0.0164 atomic percent at 1342 C.  $T_m = 1769$  C
- Palladium- 0.7 atomic percent at 1552 C, solid  
0.4 atomic percent for liquid  
high solubility, but decreases as T goes up
- Rhodium - little solubility, very low

Oxygen:

- Palladium- PdO decomposes at 750 C  
solubility is 0.63 atomic percent at 1200 C.
- Platinum - no data found
- Rhodium - dissolves a considerable amount at high temperatures. Rh<sub>2</sub>O<sub>3</sub> decomposes at 1100 C in 1 atmosphere of oxygen
- Copper - Copper and oxygen form a eutectic with low solid solubility of oxygen in copper where there was less than 0.036 atomic percent at 1000 C. the eutectic temperature is 1065 C and the eutectic (with cuprous oxide) composition is 1.5 atomic percent. There is unlimited solubility of oxygen in copper or nickel some 20 C above the eutectic temperatures.
- Nickel - Nickel and oxygen form a eutectic with increasing solubility with decreasing temperature where we have 0.044 atomic percent oxygen in the solid at 1200 C. The eutectic temperature is 1438 C, and the eutectic point is 0.87 atomic percent oxygen.

In summary then nitrogen cannot cause the observed porosity in all cases because of the variety of ambient atmospheres used. Also since the helium-hydrogen mixture contained no more than 5% hydrogen, and the overall pressure used was normally around 200 - 300 Torr, then the partial pressure of the hydrogen would be only around 0.1 to 0.2 Torr. A high solubility of

0.7 atomic percent of hydrogen in Palladium at 1 atmosphere would then give only 0.0001 atomic percent. Alternately, the solubility of hydrogen in copper liquid would only be 0.000005 atomic percent for the low partial pressure of hydrogen in the tube. So it is unlikely that raw hydrogen was solubilized by the melt. The low partial pressure of hydrogen was confirmed as well by the mass spectrometer measurements.

Since porosity was observed predominantly in the nickel samples processed in air and helium-hydrogen mixture and in the palladium samples process in air, it is a fair conclusion that the dissolved gas was oxygen, either from the atmosphere or from the oxide.

#### IX. Summary of Etching Procedures

##### 1. Chemical Polish for Copper:

After mechanical polish at 5 micron alumina or diamond grit, submerge specimen in solution for several seconds at a time until surface scratches have been removed. Use at room temperature or warmer.

Nitric Acid	30 ml
Hydrochloric Acid	10 ml
Phosphoric Acid	10 ml
Glacial Acetic Acid	50 ml

Taken from reference .

##### 2. Chemical Etchant for Copper:

Immediately after chemical polishing with procedure given above, followed by rinsing; a brief few seconds in this etchant

will reveal grain and dendrite structures. The etchant is a dilute (10%) solution of a commercially available etchant for printed circuit boards, which primarily contains ferric chloride solution.

### 3. Chemical Etchant for Nickel

Use freshly prepared for 5 to 30 seconds, thereby revealing grain boundaries in high nickel alloys. Use after mechanical polishing.

Nitric Acid	50%
Glacial Acetic Acid	50%

Taken from reference .

### 4. Chemical Etchant for Palladium

This etchant is a dilute solution of a commercially available chromic acid/sulfuric acid solution used as a glassware cleaning acid. A 5 to 10% dilution of the glass cleaner solution was found to work for palladium, where no other techniques worked. The treatment needed 30 to 60 seconds in order to work at room temperature or warmer.

### 5. Electro-etchant for Platinum, Rhodium, and Iridium

The following solution was found to be the best to reveal grain boundary structure in the above elements. A graphite cathode was used with 6 volts AC to the sample and electrode. The solution was used at room temperature and constantly stirred to

remove the adherent bubbles formed during the reaction. Often as many as 2 minutes of treatment was required for rhodium and as little as 20 seconds for platinum. Etching was performed after the mechanical polishing and etching.

Taken from reference 6.

#### 6. Specimen Cleaning - General procedure

In all cases the general procedure was to rinse the specimen with water, then with alcohol and dried with clean pressurized air between each treatment. Often considerable drying and rinsing was required to prevent acid trapped in pores in the specimen from attacking the surface when it subsequently exits from the specimen.

## BIBLIOGRAPHY

1. Ellingham, H.T.T., Jour. Soc. Chem. Ind. (London) 63, 125 (1944).
2. Swalin, Richard A., Thermodynamics of Solids; Wiley & Sons, New York (1972).
3. Barin, I., O. Knacke, and O. Kubaschewski, Thermochemical Properties of Inorganic Substances; Springer-Verlag, Berlin (1973).
4. Barin, I., O. Knacke, and O. Kubaschewski, Thermochemical Properties of Inorganic Substances Supplement; Springer-Verlag, Berlin (1977).
5. Lupis, C.H.P., Chemical Thermodynamics of Materials; North-Holland, New York (1983).
6. Petzoe, G., "Metallographic Etching", American Society for Metals, Metals Park (1978).
7. Smithells, C.J., "Gases and Metals", London, 1937.

TABLE I

Summary of Drop Tube Specimens

Legend: pee: picture, electro-etched  
 pe: picture, chemically etched  
 pr: picture, real surface (light microscopy)  
 sem: scanning electron microscope  
 C: cooling curve

ID#	Material	Initial Weight	Final Weight	Comments
NT221	Rh			High purity, e-beam, pee
NT224	Rh			High purity, e-beam, mounted not etched
NT227	Rh			High purity, e-beam, mounted not etched
NT228	Rh			High purity, e-beam, mounted not etched
NT269	Rh			High purity, pee
NT339	Cu			Electrical wire, not mounted
NT344	Cu			High purity, He+H atmos, dropped into Al foil, pe
NT346	Pd			Arced and splattered, not mounted
NT349	Cu			High purity, He+H atmos, C
NT351	Cu			High purity, He+H in tube; C. Ar in bell jar, dirty, pe
NT357	Cu			Air in bell jar, C, He+H in tube, air in catch tube
NT417	Pd	316.99	316.43	pe
NT420	Pd	338.63	321.25	pe
NT422	Pd	190.83		splattered
NT426	Ni	252.43	252.81	He atmos, pr, pe, sem
NT427-8	Ni	250.0	248.03	He atmos, pe
NT434	Cu			He+H atmos, not totally melted, pe
NT435	Cu			He+H atmos, not totally melted, pe
NT446	Ni	229.48	300.0	He+H, pe, C
NT447	Ni	300.15	300.16	He+H atmos, pe, C
NT448	Ni	213.43	213.57	He+H atmos, rainy day, sem, pe
NT449	Ni	249.28	294.47	He+H atmos, rainy day, sem, pe
NT450	Pd	335.36	334.12	He+H atmos, rainy day, pe, sem
NT451	Pd	351.61	334.12	He+H atmos, rainy day, splatted

TABLE I. (cont.)

ID#	Material	Initial Weight	Final Weight	Comments
NT452	Pd	371.32		He+H atmos, pe
NT453	Ni	358.74	360.0	Air, pe, C
NT454	Ni	350.0	342.94	Air, pe, C
NT455-6	Ni	295.9		No melt in air
NT457	Cu			Air splat, C
NT458	Cu			Air splat, C
NT459	Pd	360.5		Air, pe
NT460	Pd	372.88		Air, pe, C
NT461	Pd	387.77		Air, pr, pe, sem
NT462	Pd	393.32		Air, pe
NT463	Cu			Air splat, C
NT464	Cu			Air splat, C
NT465	Cu			Vacuum splat, C
NT468	Pd			Vacuum splat, C
NT469	Pd	311.23		He+H atmos, pe
NT470	Pd	323.39		He+H atmos, pe
NT472	Cu			He+H atmos, pe
NT474	Cu			High purity, He+H atmos, pe
NT559	Ni	374.03		Vacuum, pe, C
NT560	Ni	285.24		Vacuum, sem, pe, C
NT577	Cu	240.14	238.78	He+H atmos, in- complete melt, not mounted
NT578	Cu	232.25	230.8	He+H atmos, fell from coil, not mounted
NT581	Cu	244.30	240.31	He+H atmos, not mounted
NT582	Cu	189.10	185.98	He+H atmos
NT583	Cu	184.89	183.07	He+H atmos, not mounted
NT584	Cu	268.30		He+H atmos, not high purity, not mounted
NT585	Cu		231.77	He+H atmos, half splat, data as NT584
NT586	Cu		233.77	He+H atmos, elongated half splat, test
NT587	Cu	177.89	176.14	He+H atmos, incomplete melt, not mounted
NT589	Ni	371.30	371.00	He+H atmos
NT590	Ni	380.74	380.74	He+H atmos

TABLE I. (cont.)

ID#	Material	Initial Weight	Final Weight	Comments
NT591	Pd	269.02	258.51	He+H atmos, pe
NT592	Pd	196.76	189.19	He+H atmos, pe
NT594	Cu	163.73	162.54	He+H atmos, not levitated, not mounted
NT624	Pt			E-beam, vacuum, pee, C
NT625	Rh			E-beam, no data, pee
NT627	Pt			E-beam, incomplete melt, not mounted, C
NT630	Pt			E-beam, pee
NT657	Pt		65.4	E-beam, no data
NT659	Pt		50.23	E-beam, wire sample, C
NT661	Pt		24.28	E-beam, no data, not mounted
NT662	Rh		20.61	E-beam, irregu- lar shape, may have wire in it, C
NT663	Pt		59.3	E-beam, wire imbedded in it, C
NT664	Rh		23.2	E-beam, wire imbedded in it, C
NT665	Rh		30.7	E-beam, may have wire imbedded in it
NT670	Ir		76.81	E-beam, wire imbedded in it
NT671	Ir		33.92	E-beam, may have wire imbedded in it

TABLE II.

Summary of Drop Tube Specimen Grain Size

Sample Number	Element	Atmosphere	Grain Size (cm)	Standard Dev. (cm)
NT221	Rh	E-beam	.0171	.0076
NT269	Pd	E-beam	.0131	.0035
NT344	Cu	He+H	.0969	.0031
NT351	Cu	He+H	.0252	.0175
NT448	Ni	He+H	.0252	.0103
NT449	Ni	He+H	.0297	.0102
NT452	Pd	He+H	.0184	.0093
NT453	Ni	Air	.0163	.0048
NT454	Ni	Air	.0304	.0105
NT460	Pd	Air	.0056	.0022
NT461	Pd	Air	.0056	.0022
NT462	Pd	Air	.0059	.0019
NT470	Pd	He+H	.0221	.0078
NT474	Cu	He+H	.0236	.0084
NT560	Ni	Vacuum	.0143	.0071
NT582	Cu	He+H	.0249	.0118
NT585	Cu	He+H	.0074	.0037
NT586	Cu	He+H	.0246	.0136
NT589	Ni	He+H	.0192	.0088
NT590	Ni	He+H	.0223	.0119
NT591	Pd	He+H	.0151	.0057
NT592	Pd	He+H	.0111	.0061
NT625	Rh	E-beam	.0044	.0024
NT630	Pt	E-beam	.0085	.0021

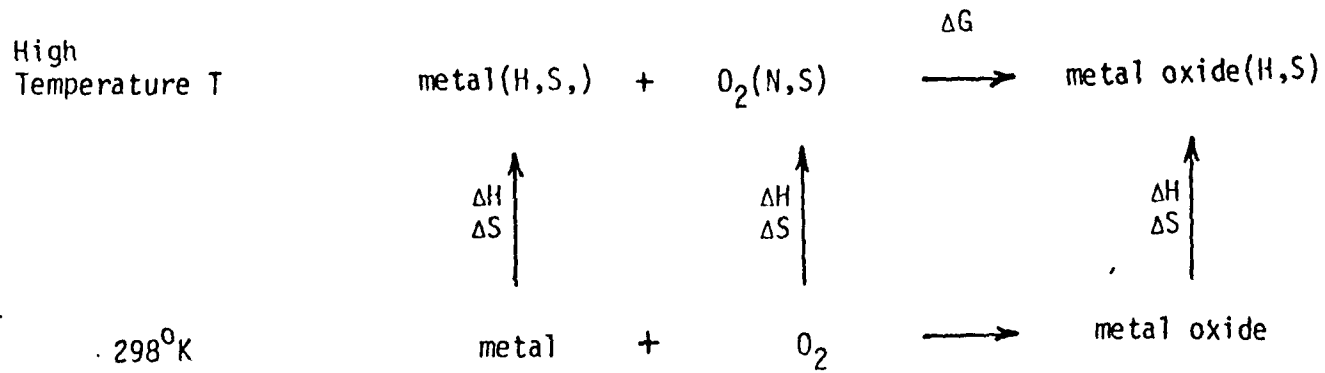
TABLE III.

Summary of Dendrite size Measurements

Sample Number	Element	Dendrite Size (cm)	Standard Deviation
NT417	Pd	0.0066	0.0023
NT420	Pd	0.0086	0.0021
NT427-8	Ni	0.0030	0.0008
NT460	Pd	0.0056	0.0022
NT461	Pd	0.0056	0.0022
NT462	Cu	0.0059	0.0019
NT474	Cu	0.0111	0.0042
NT582	Cu	0.0070	0.0014
NT624	Pt	0.0011	0.0004
NT625	Rh	0.0024	0.0006



Figure 2. Thermochemical calculations for Richardson charts



$$H(T) = \Delta H_{298}^{\circ} + \Delta H \quad \text{where} \quad \Delta H = \int_{298}^T c_p \, dT + \sum_{i=1}^n H_i$$

$$S(T) = \Delta S_{298}^{\circ} + \Delta S \quad \text{where} \quad \Delta S = \int_{298}^T c_p/T \, dt + \sum_{i=1}^n H_i/T$$

$$\Delta H(T) = H(\text{metal oxide}) - H(\text{metal}) - H(\text{O}_2)$$

$$\Delta S(T) = S(\text{metal oxide}) - S(\text{metal}) - S(\text{O}_2)$$

$$\Delta G(T) = \Delta H - T \Delta S = RT \log P_{\text{O}_2}$$

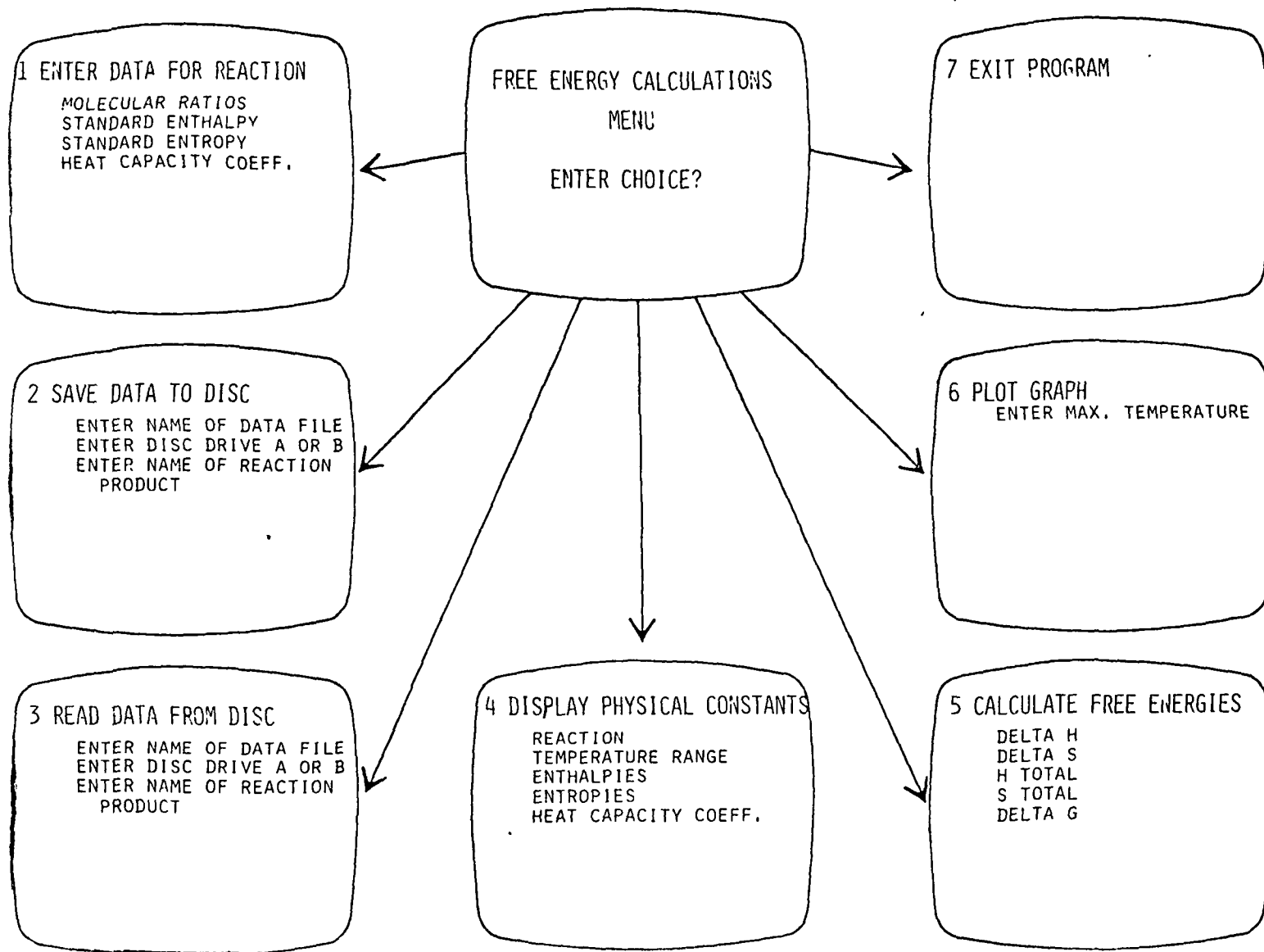


Figure 3. Menu driven program flow nodes for easy user interface

REACTION	2 NI	+	O2	---	2 NIO
TEMPERATURE RANGE 1 IS	25	TO	252	DEGREES C	
ENTHALPY	0		0		-57500
ENTROPY	7.14		49		9.100001
HEAT CAPACITY COEFFICIENTS					
A	7.8		7.02		-4.99
B	-.43		0		37.58
C	-1.335		0		3.89
D	0		0		0
AT 252 DEGREES C PHASE TRANSITION VALUES ARE					
ENTHALPY	140		0		0
ENTROPY	.222		0		0

ORIGINAL PAGE IS  
OF POOR QUALITY

ENTER <CR> TO GET NEXT DATA OR <X> & <CR> TO GO TO MENU? █

Figure 4. Thermochemical constants for first temperature range

REACTION	2 NI	+	O2	---	2 NIO
TEMPERATURE RANGE	2 IS	253	TO	292	DEGREES C
ENTHALPY	0		0		-57500
ENTROPY	7.14		49		9.100001
HEAT CAPACITY COEFFICIENTS					
A	7.1		7.02		13.88
B	1		0		0
C	-2.23		0		0
D	0		0		0
AT 292 DEGREES C PHASE TRANSITION VALUES ARE					
ENTHALPY	4200		0		0
ENTROPY	2.436		0		0

ENTER <CR> TO GET NEXT DATA OR <X> & <CR> TO GO TO MENU? 

Figure 5. Thermochemical constants for second temperature range

REACTION            2 NI   +    O2        --->    2 NiO

TEMPERATURE RANGE 3 IS 293 TO 1984 DEGREES C

ENTHALPY            0                    0                    -57500

ENTROPY             7.14                49                   9.100001

HEAT CAPACITY COEFFICIENTS

A                    9.3                   7.02                11.18

B                    0                    0                    2.02

C                    0                    0                    0

D                    0                    0                    0

AT 1984 DEGREES C PHASE TRANSITION VALUES ARE

ENTHALPY            0                    0                    0

ENTROPY             0                    0                    0

ORIGINAL PAGE IS  
OF POOR QUALITY

ENTER <CR> TO GET NEXT DATA OR <X> & <CR> TO GO TO MENU? █

Figure 6. Thermochemical constants for third temperature range

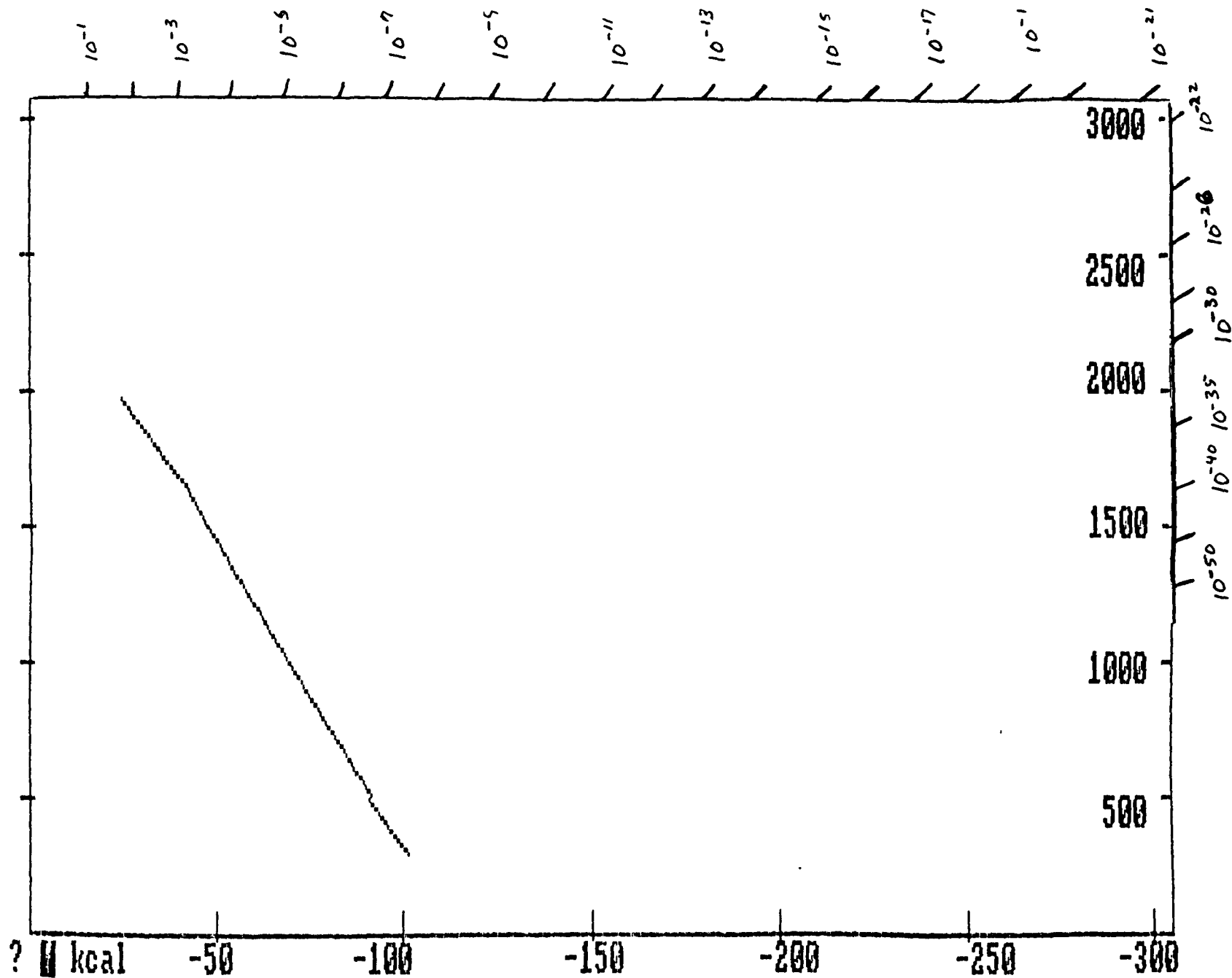
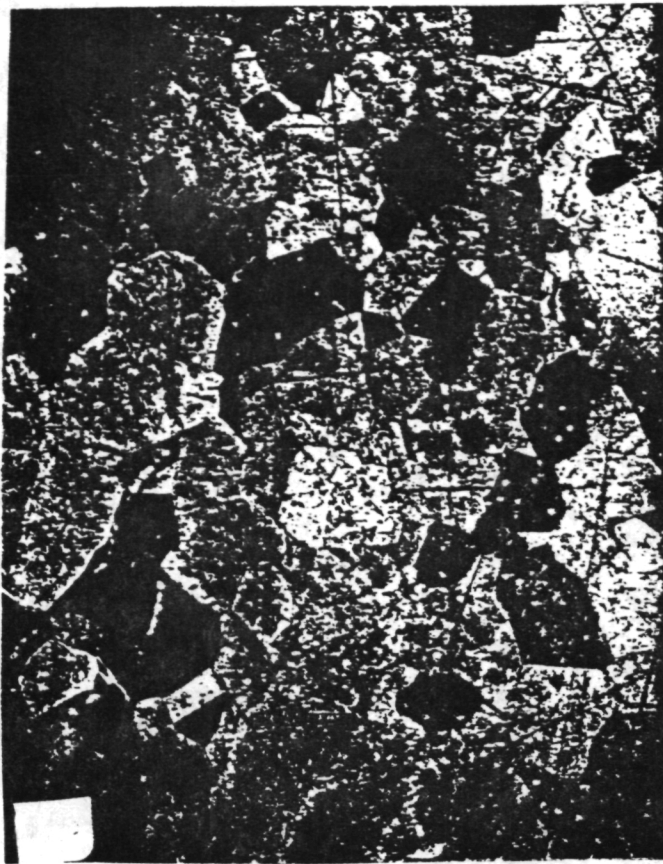


Figure 7. Ellingham chart for  $N_2O$  from IBM  
 PC screen dump with overlaid  $10_2$  scale



Pd, NT591  
65X

ORIGINAL PAGE IS  
OF POOR QUALITY



Pd, NT592  
65X

Figure 8. Photomicrographs of two Palladium drops. Data is given in Table 1



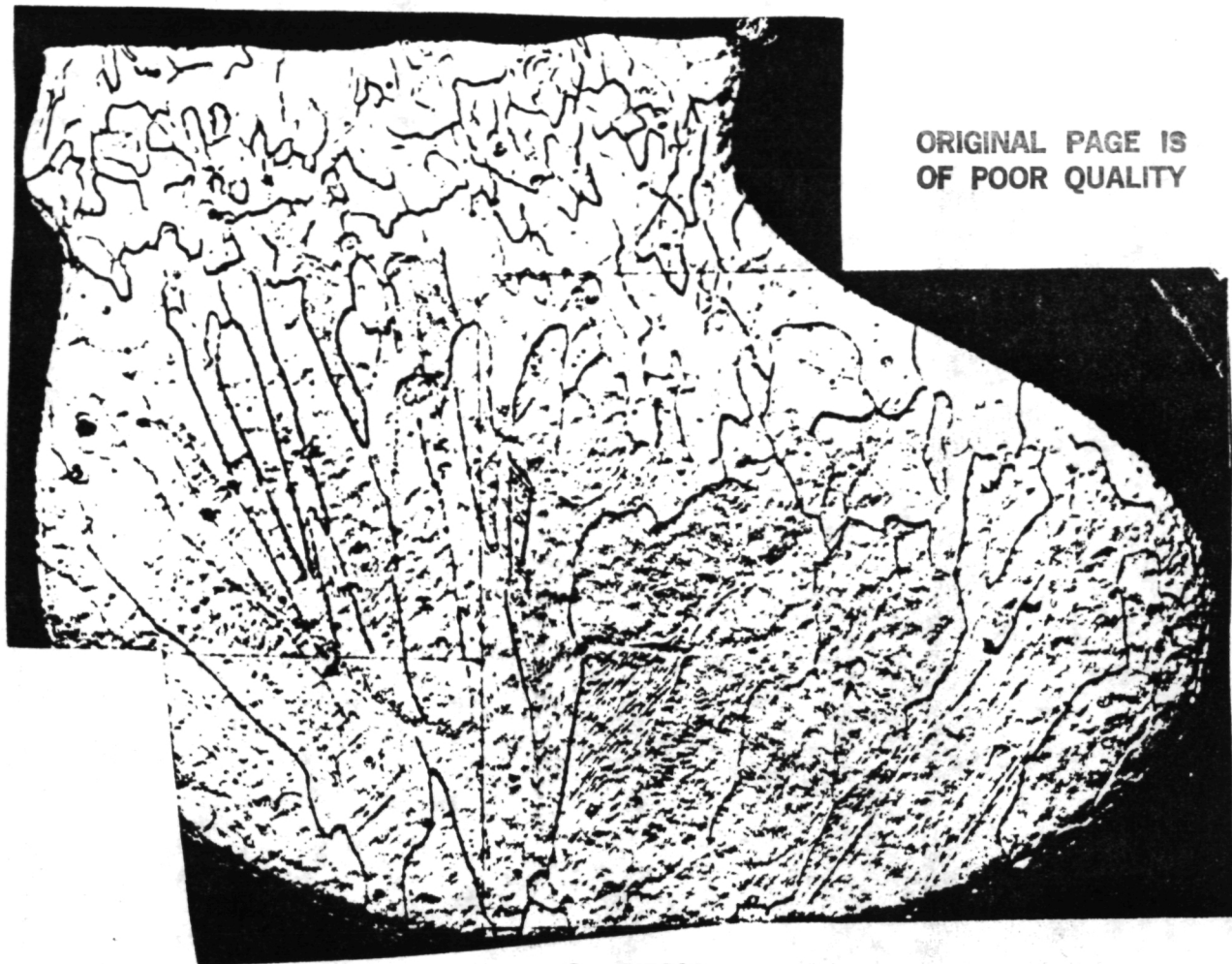
Ni, NT590  
65X



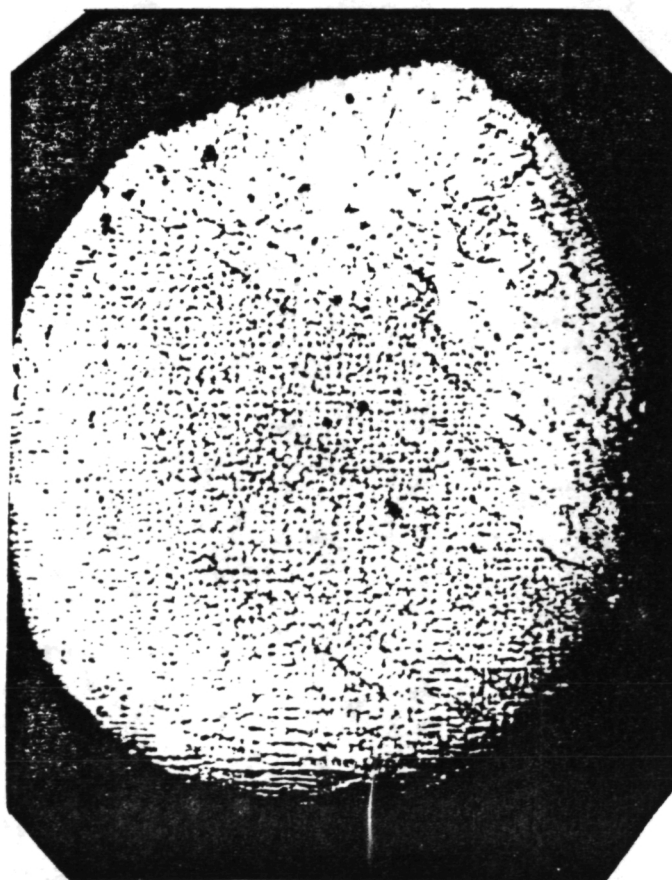
Ni, NT448  
65X

Figure 9. Photomicrograph of two different Nickel drop specimens. Data is given in Table I.

ORIGINAL PAGE IS  
OF POOR QUALITY



Cu, NT585  
65X



Ni, NT427-8  
40X

Figure 10

Photomicrographs of  
two unique specimens,  
copper and nickel  
Data is summarized  
in Table I

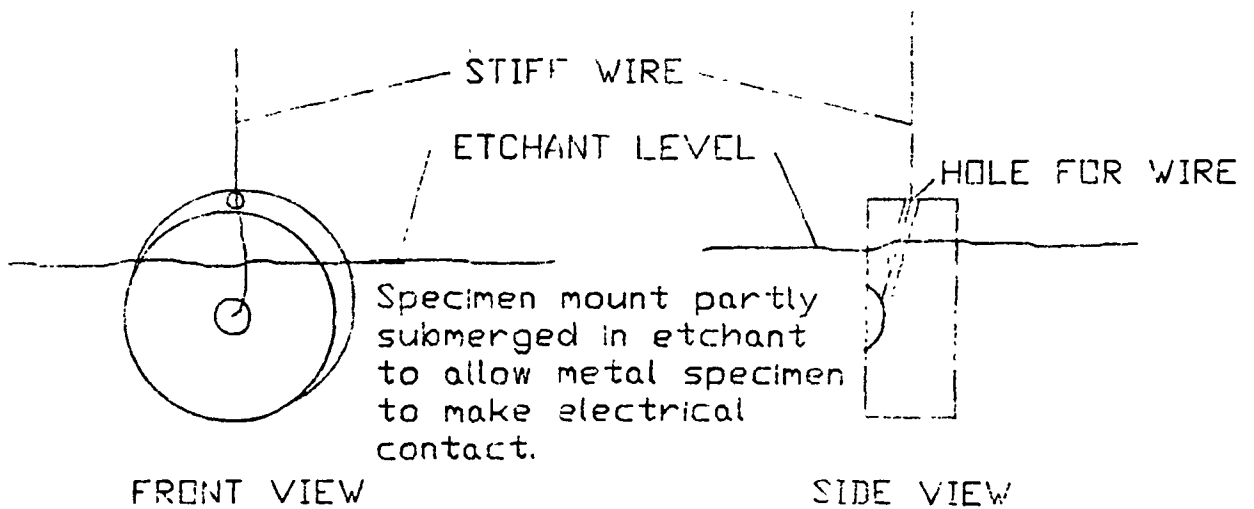
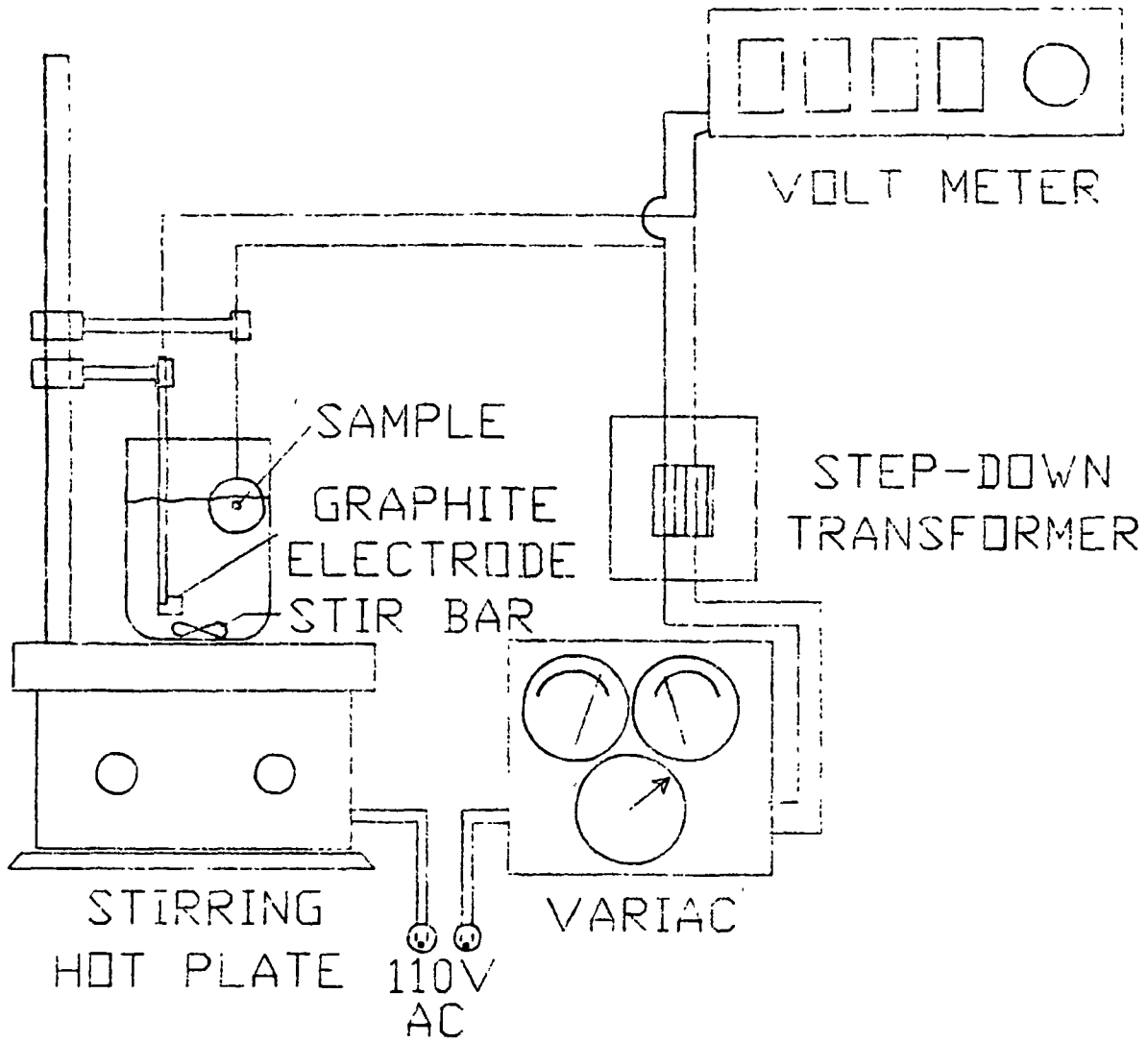


Figure 11. Electro-etching apparatus constructed for this work

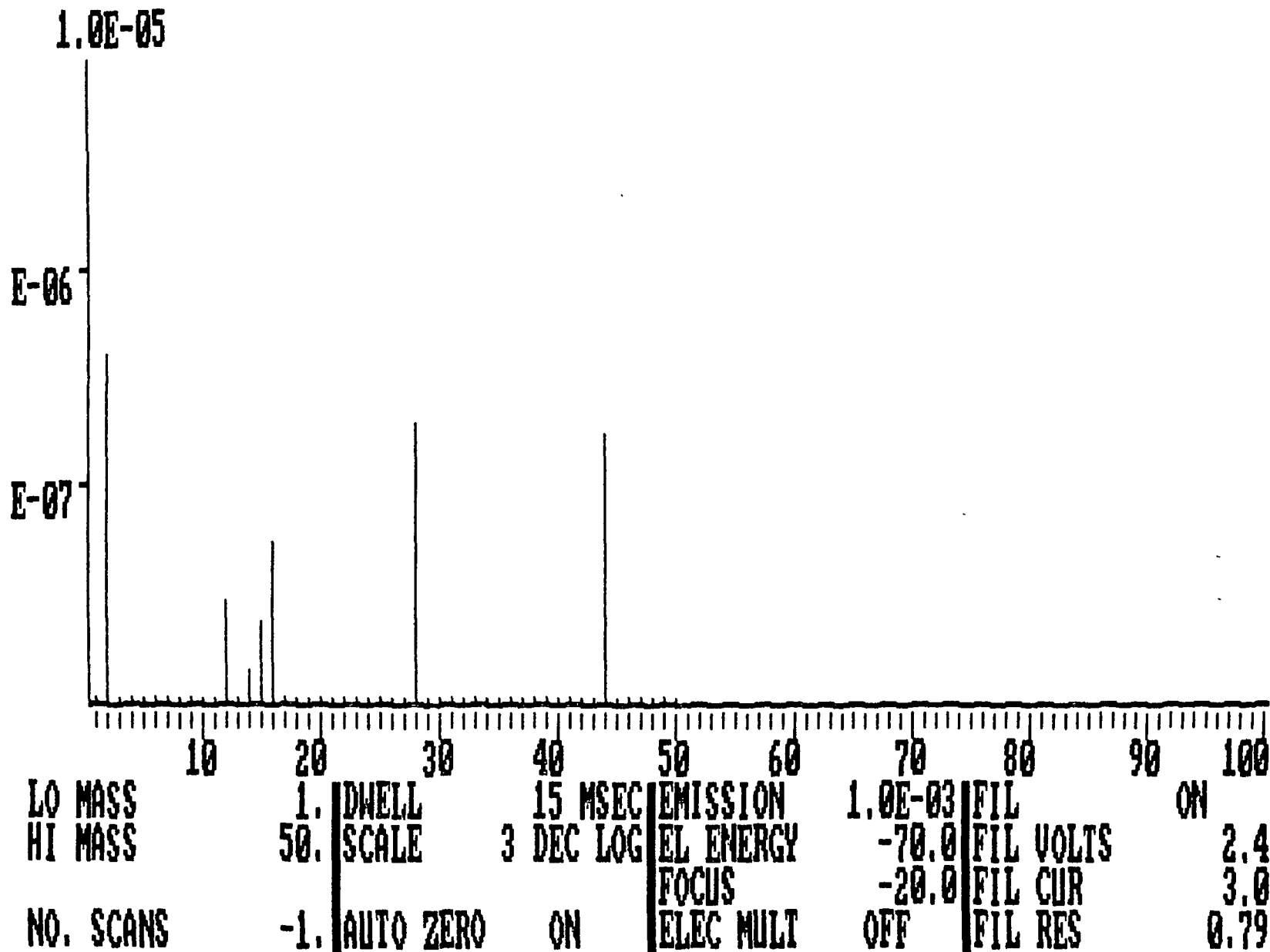


Figure 12. Mass spectrum using Dycor system and subtraction of background feature.

## APPENDIX A

## Appendix A.

### FREE ENERGY PROGRAM written in Microsoft BASICA for the IBM Personal Computer

Comments: This program has been written with a menu driven user interface for ease of use. Each task such as enter data, read data from the disk, calculate free energies to a specified temperature, or to plot data is determined through a primary menu.

```
9 REM SET-UP AND PRIMARY MENU
10 DIM C$(3),M(3),H(3),S(3),A(3,9,4),HP(3,5),SP(3,5)
20 DIM TP(20)
30 KEY OFF
100 CLS
110 PRINT:PRINT
120 PRINT TAB(20);"FREE ENERGY CALCULATIONS MENU"
130 PRINT
140 PRINT:PRINT TAB(5);"1 ENTER DATA FOR A REACTION"
150 PRINT:PRINT TAB(5);"2 SAVE DATA TO DISK"
160 PRINT:PRINT TAB(5);"3 READ DATA FROM DISK"
170 PRINT:PRINT TAB(5);"4 DISPLAY PHYSICAL CONSTANTS"
180 PRINT:PRINT TAB(5);"5 CALCULATE FREE ENERGIES"
190 PRINT:PRINT TAB(5);"6 PLOT ONE REACTION"
200 PRINT:PRINT TAB(5);"7 PLOT SEVERAL REACTIONS"
210 PRINT:PRINT TAB(5);"8 EXIT PROGRAM"
220 PRINT:INPUT "ENTER CHOICE"; C
230 ON C GOSUB 300,600,900,1100,1300,2500,3500,250
240 GOTO 100
250 STOP

298 REM THE DATA ENTRY SUBROUTINE WITH DATA ENTERED FROM TABLES IN 299
REM THE REFERENCE TABLES OF BARIN, ET AL.
300 CLS
310 INPUT "enter metallic reactant ";C$(1)
315 INPUT "enter molecular ratio ";M(1)
320 INPUT "enter gaseous reactant ";C$(2)
325 INPUT "enter molecular ratio ";M(2)
330 INPUT "enter reaction product ";C$(3)
335 INPUT "enter molecular ratio ";M(3)
340 FOR I = 1 TO 3
350 CLS
360 PRINT "enter data for "; C$(I)
370 INPUT "enter standard enthalpy at 25 degrees C ";H(I)
375 INPUT "enter standard entropy at 25 degrees C ";S(I)
380 INPUT "enter number of phases";N(I)
384 FOR J = 1 TO N(I)
390 INPUT "enter upper temperature ";T2(I,J)
395 PRINT
430 PRINT
440 PRINT "enter heat capacity coefficients A,B,C,D for ";C$(I)
450 INPUT "enter A coefficient";A
460 INPUT "enter B coefficient ";B
470 INPUT "enter C coefficient";C
```

```

480 INPUT "enter D coefficient";D
490 A(I,J,1)=A:A(I,J,2)=B:A(I,J,3)=C:A(I,J,4)=D
495 PRINT
500 INPUT "enter 'N' if no phase change occurs at upper
temperature";N$
510 IF N$ = "N" THEN 540
520 INPUT "enter enthalpy change at phase change temperature ";HP(I,J)
530 INPUT "enter entropy change at phase transition ";SP(I,J)
540 NEXT J
550 NEXT I
560 RETURN
600 CLS
610 F$="DATA":INPUT "ENTER NAME OF DATA FILE ";F$
620 INPUT "ENTER DISK DRIVE A OR B";D$
630 FILE$ = D$+" "+F$+".DAT"
640 OPEN FILE$ FOR APPEND AS #1
660 FOR I=1 TO 3
670 WRITE #1,C$(I),M(I),N(I),H(I),S(I)
680 FOR J = 1 TO N(I)
690 WRITE #1,T2(I,J),A(I,J,1),A(I,J,2),A(I,J,3),A(I,J,4)
700 WRITE #1,HP(I,J),SP(I,J)
710 NEXT J
720 NEXT I
730 CLOSE 1
740 RETURN

899 REM RETRIEVE DATA FROM DISK
900 CLS
910 F$= "DATA":PRINT "ENTER NAME OF DATA FILE ";:INPUT F$
920 FILE$ = F$+".DAT"
940 INPUT "ENTER NAME OF REACTION PRODUCT ";R$
950 OPEN FILE$ FOR INPUT AS #1
960 IF EOF(1) THEN 1060
980 FOR I = 1 TO 3
990 INPUT #1,C$(I),M(I),N(I),H(I),S(I)
1000 FOR J = 1 TO N(I)
1010 INPUT #1,T2(I,J),A(I,J,1),A(I,J,2),A(I,J,3),A(I,J,4)
1020 INPUT #1,HP(I,J),SP(I,J)
1030 NEXT J
1040 NEXT I
1050 IF C$(3) = R$ THEN 960
1060 CLOSE 1
1070 GOSUB 3000
1080 RETURN

1099 REM THIS ROUTINE PRINTS THE THERMODYNAMIC VALUES
1100 FOR J = 1 TO PMAX
1110 CLS
1120 PRINT "REACTION",M(1);C$(1);" + "C$(2);"
";M(3);C$(3)
1125 PRINT:PRINT
1130 PRINT "ENTHALPY",H(1),H(2),H(3)
1135 PRINT
1140 PRINT "ENTROPY",S(1),S(2),S(3)

```

ORIGINAL PAGE IS  
OF POOR QUALITY

```
1145 PRINT :PRINT
1150 PRINT "TEMPERATURE RANGE ";J;" IS ";TP(J); " TO ";TP(J+1); "
DEGREES C"
1155 PRINT :PRINT
1160 PRINT "HEAT CAPACITY COEFFICIENTS"
1170 PRINT "A", AX(1,J,1),AX(2,J,1),AX(3,J,1)
1180 PRINT "B", AX(1,J,2),AX(2,J,2),AX(3,J,2)
1190 PRINT "C", AX(1,J,3),AX(2,J,3),AX(3,J,3)
1200 PRINT "D", AX(1,J,4),AX(2,J,4),AX(3,J,4)
1205 PRINT
1220 PRINT "ENTHALPY",HX(1,J),HX(2,J),HX(3,J)
1230 PRINT "ENTROPY", SX(1,J),SX(2,J),SX(3,J)
1240 LOCATE 24,5
1250 INPUT "ENTER <CR> TO GET NEXT DATA OR <X> & <CR> TO GO TO
MENU":A$
1260 IF A$ = CHR$(88) THEN RETURN
1270 NEXT J
1280 RETURN

1299 REM THIS SUBROUTINE CALCULATE THE DELTA G VALUES
1300 CLS
1310 LPRINT "REACTION",M(1);C$(1);" + " ;C$(2)" -->
";M(3);C$(3)
1320 LPRINT:LPRINT "TEMP","DELTA H","DELTA S","DELTA G"
1340 T1A = T1(1) + 273
1360 INPUT "ENTER MAXIMUM TEMPERATURE FOR THIS CALCULATION"; TMAX
1370 FOR T2A = T1A TO TMAX + 273 STEP 50
1380 GOSUB 2000
1390 LPRINT T2A,HREACT,SREACT,GT2
1400 NEXT T2A
1480 PRINT "MOLAR ENTHALPIES ARE ";HTOTAL(1),HTOTAL(2),HTOTAL(3)
1490 PRINT "MOLAR ENTROPIES ARE "; STOTAL(1),STOTAL(2),STOTAL(3)
1550 PRINT "THE FREE ENERGY AT ";TMAX;" DEGREES C IS
";GT2;"CAL/";M(3);"MOLE
1560 PRINT
1580 INPUT "ENTER <CR> TO RETURN TO MENU OR <PrtSc> TO PRINTER "; X$
1590 RETURN

1999 REM THIS SUBROUTINE PERFORMS THE SUMMATION OVER THE COEFFICIENTS
2000 FOR I = 1 TO 3
2010 HS(I) = H(I):SS(I) = S(I)
2020 T1A = TP(J) + 273
2030 HS(I) = HS(I) + HX(I,J-1):SS(I) = SS(I) + SX(I,J-1)
2050 HCAPA(I) = AX(I,J,1) * (T2A-T1A)
2060 HCAPB(I) = AX(I,J,2) * .5 * 10^-3 * (T2A*T2A-T1A*T1A)
2070 HCAPC(I) = AX(I,J,3) * 10^-5 * (1/T1A - 1/T2A)
2080 HCAPD(I) = AX(I,J,4) * .333 * 10^-6 * (T2A*T2A*T2A - T1A*T1A*T1A)
2090 HTOTAL(J) = HS(J) + HCAPA(I)+ HCAPB(I) + HCAPC(I) + HCAPD(I)
2100 ENTRA(I) = AX(I,J,1) * LOG(T2A/T1A)
2110 ENTRB(I) = AX(I,J,2) * 10^-3 * (T2A-T1A)
2120 ENTRC(I) = AX(I,J,3) * 10^-5 * (2*(T1A^-2 - T2A^-2))
2130 ENTRD(I) = AX(I,J,4) * .5 * 10^-6 * (T2A*T2A-T1A*T1A)
2140 STOTAL(I) = SS(I) + ENTRA(I)+ ENTRB(I) + ENTRC(I) + ENTRD(I)
2150 NEXT I
```

```
2160 HREACT = M(3)*HTOTAL(3) - M(1)*HTOTAL(1) - HTOTAL(2)
2170 SREACT = M(3)*STOTAL(3) - M(1)*STOTAL(1) - STOTAL(2)
2180 GT2 = HREACT - T2A*SREACT
2190 RETURN
```

```
2498 REM THIS SUBROUTINE PERFORMS THE GRAPHICAL TASKS FOR A SINGLE
2499 REM REACTION
2500 CLS
2510 INPUT "ENTER MAXIMUM TEMPERATURE FOR THIS CALCULATION"; TMAX
2520 GOSUB 4000
2530 TSC = 180/3000
2540 FESC = 600/300000
2550 T1A = TP(1) + 273
2560 HGRD = M(3)*H(3) - M(1)*H(1) - H(2)
2570 SGRD = M(3)*S(3) - M(1)*S(1) - S(2)
2580 GRFE = HGRD - T1A*SGRD
2590 STEMP = 190 - T1A*TSC
2600 SFE = 10 - GRFE*FESC
2610 PSET (SFE,STEMP)
2615 FOR J = 1 TO PMAX
2620 FOR T2A = TP(J) + 273 TO TP(J+1) + 273 STEP 50
2625 IF T2A > TMAX THEN 2680
2630 GOSUB 2000
2640 TCOR = 190 - T2A*TSC
2650 FECOR = 10 - GT2*FESC
2660 LINE -(FECOR,TCOR)
2670 NEXT T2A
2675 NEXT J
2680 LOCATE 25,1
2690 INPUT X#
2700 RETURN
```

```
2999 SUBROUTINE TO SORT THERMODYNAMIC ENTRIES ACCORDING TO TEMPERATURE
3000 TP(1)=25;K = 2
3010 FOR I = 1 TO 3
3020 FOR J = 1 TO N(I)
3030 TP(K) = T2(I,J)
3040 K = K + 1
3050 NEXT J
3070 NEXT I
3080 PMAX = K - 1
3090 D = 0
3100 FOR I = 1 TO PMAX-1
3110 FOR K = I + 1 TO PMAX
3120 IF TP(I) < TP(K) THEN 3150
3130 IF TP(I) = TP(K) THEN TP(K) = 99999!:GOTO 3150
3140 SWAP TP(I),TP(K)
3150 NEXT K
3160 NEXT I
3170 FOR I = 1 TO PMAX
3180 IF TP(I) = 99999! THEN D = D + 1
3190 NEXT I
3200 PMAX = PMAX - D
3220 FOR I = 1 TO 3
```

ORIGINAL PAGE IS  
OF POOR QUALITY

```
3230 J = 1
3240 FOR K = 1 TO PMAX
3260 FOR C = 1 TO 4:AX(I,K,C) = A(I,J,C):NEXT C
3270 IF TP(K+1) < T2(I,1) THEN HX(I,K)=0: SX(I,K) = 0:GOTO 3290
3280 HX(I,K) = HP(J,J):SX(I,K) = SP(J,J)
3290 IF TP(K+1) >= T2(I,J) THEN J=J+1
3300 NEXT K
3310 NEXT J
3315 STOP
3320 RETURN

3499 REM SUBROUTINE TO GRAPH SEVERAL REACTIONS ON ONE GRAPH
3500 CLS
3510 F$= "DATA":PRINT "ENTER NAME OF DATA FILE ";;INPUT F$
3520 INPUT "ENTER DISK DRIVE A OR B";D$
3530 FILE$ = D$+" "+F$+".DAT"
3540 FOR CMP = 1 TO 10
3550 PRINT "ENTER REACTION PRODUCT OR 0 FOR NONE";CMP;;INPUT RP$(CMP)
3560 IF RP$(CMP) = "0" THEN 3580
3570 NEXT CMP
3580 NUM = CMP - 1
3590 INPUT "ENTER MAXIMUM TEMPERATURE FOR THESE CALCULATIONS"; TMAX
3600 GOSUB 4010
3610 TSC = 180/3000
3620 FESC = 600/300000
3630 FOR CMP = 1 TO NUM
3640 R$= RP$(CMP)
3650 GOSUB 950
3660 T1A = TP(1) + 273
3670 HGRD = M(3)*H(3) - M(1)*H(1) - H(2)
3680 SGRD = M(3)*S(3) - M(1)*S(1) - S(2)
3690 GRFE = HGRD - T1A*SGRD
3700 STEMP = 190-T1A*TSC
3710 SFE = 10-GRFE*FESC
3720 FSET (SFE,STEMP)
3730 FOR T2A = T1A + 50 TO TMAX + 273 STEP 50
3740 GOSUB 2000
3750 TCOR = 190-TSC*T2A
3760 FECOR = 10-FESC*GT2
3770 LINE -(FECOR,TCOR)
3780 NEXT T2A
3790 NEXT CMP
3800 LOCATE 25,1
3810 INPUT X$
3820 RETURN

3999 REM SUBROUTINE FOR GENERATING GRAPHIC FORM ON IBM PC SCREEN
4000 T$="          -50          -100 (local) -150          -200 -250
-300 "
4010 CLS
4020 SCREEN 2
4030 LINE (10,5)-(620,190),,B
4040 FOR Y = 1 TO 6
4050 LINE (5,190-Y*30)-(12,190-Y*30)
```

4060 LINE (615,190-Y\*30)-(620,190-Y\*30)

4070 YV = Y\*500

4080 LOCATE 25-Y\*3.9,73:PRINT USING "####";YV

4090 NEXT Y

4100 T\$=" local -50 -100 -150 -200 -25  
-300 "

4110 FOR X = 1 TO 6

4120 LINE (10+X\*100,195)-(10+X\*100,185)

4130 NEXT X

4140 LOCATE 25,1:PRINT T\$;

4150 RETURN